

Supporting Information

Porous aromatic cage-based electrochemical sensor for enantioselective recognition of DOPA

Junning Kou^{a1}, Ziyu Zhu^{a1}, Jianzhu Jiang^{a1}, Li Chen^b, Kunhao Zhang,^{c}*

Guogang Shan^{a}, Xinlong Wang^{a*}, Zhongmin Su^b, Chunyi Sun^{a*}*

- a. National & Local United Engineering Laboratory for Power Battery, Department of Chemistry, Northeast Normal University, Changchun, Jilin, 130024, China.*
- b. Department of Chemistry, Faculty of Science, Yanbian University, Yanji, Jilin, 133002, China.*
- c. Shanghai Synchrotron Radiation Facility (SSRF), Shanghai Advanced Research Institute, Chinese Academy of Sciences, Shanghai, 201204, China*

¹ These authors contributed equally.

* Corresponding author.

E-mail address: suncy009@nenu.edu.cn (C. Sun); wangxl824@nenu.edu.cn (X. Wang); shangg187@nenu.edu.cn (G. Shan); zhangkh@sari.ac.cn (K. Zhang)

Table of Contents

Experimental Procedures	3
Results and Discussion	4
Fig. S1. FTIR spectrum of $C_{60}@R$ -PAC-2 after soaking under different conditions.	4
Fig. S2. Photograph of the prepared crystals of $C_{60}@R$ -PAC-2.....	4
Fig. S3. PXRD patterns of cages.	5
Fig. S4. PXRD patterns of $C_{60}@R$ -PAC-2 under different harsh conditions.	5
Fig. S5. UV-vis diffuse reflectance spectra of R -PAC-2 and $C_{60}@R$ -PAC-2.	6
Fig. S6. UV absorption spectra of the solution after different solution after immersing $C_{60}@R$ -PAC-2.	6
Fig. S7. DPV of GCE, C_{60}/GCE , PAC-2/GCE and MIX in 0.01 M PBS solution containing 0.1 mM D-Dopa or L-Dopa.	7
Fig. S8. Repeated electrochemical recognition of DOPA enantiomers by using $C_{60}@R$ -PAC-2/GCE electrode.....	7
Fig. S9. The stability of the $C_{60}@R$ -PAC-2/GCE sensor was studied after storing for 1 week.....	8
Fig. S10. DPV curves of increased concentrations (30 - 1000 μ M) of enantiomers D-DOPA and L-DOPA at the $C_{60}@R$ -PAC-2/GCE electrode.....	8
Fig. S11. DPV curves of increased concentrations (30 - 1000 μ M) of enantiomers D-DOPA and L-DOPA at the $C_{60}@S$ -PAC-2/GCE electrode.	9
Fig. S12. The detection performance of chiral sensor $C_{60}@R$ -PAC-2 for interfering organic molecules.	9
Supplementary Table 1. Summary of DOPA Chiral Sensors	10
Supplementary References	11

Experimental Procedures

General information

All reagents and solvents were obtained from commercial sources and used without further purification. Fourier transform infrared (FT-IR) spectra (KBr pellets) were recorded in the range 4000–400 cm^{-1} on Nicolet 6700 using the KBr pellet method. UV-Vis spectra were recorded at a UV-Vis-NIR spectrophotometer (Hitachi U-3900).

Synthesis of $\text{C}_{60}@R/S\text{-PAC-2}$.

R/S-Br-BINAM (0.066 g, 0.15 mmol), TFP (0.021 g, 0.1 mmol), fullerene C_{60} (0.01 mmol), *O*-Xylene (5 mL), *n*-butanol (1 mL) and 6M acetic acid (0.6 mL) were combined in a 20 mL Teflon reactor, sealed, and heated to 120°C for 84 h. After cooling in air to room temperature, the resulting crystals were filtered and repeatedly washed with Ethyl ether.

Electrochemical experiments

A bare glass carbon electrode (GCE) with a radius of 3 mm was polished continuously on a chamois for 60 s and then rinsed with deionised water. A total of 1 mg of samples, 200 μL ethanol and 100 μL of Nafion solution (5 wt%) were first dispersed in 200 μL of water to produce a suspension. Following a 30-minute sonication-assisted treatment, the homogeneous sample suspensions were loaded onto GCE. The experiments electrochemical tests were conducted on a CHI-760E electrochemical workstation and a Biologic VMP3 electrochemical workstation with a three-electrode configuration. An Ag/AgCl (saturated KCl) electrode and a Pt were used as a reference electrode and counter-electrode respectively; GCE loaded with samples were used as working electrodes.

Electrochemical Chiral Recognition of Analyte Enantiomers.

Electrochemical chiral recognition of analyte enantiomers was investigated by differential pulse voltammetry (DPV). The as-prepared chiral electrodes were placed into 5 mL test fluid. Then, DPVs were recorded from 0.0 to 0.7 V, with a step potential of 4 mV and an amplitude of 50 mV. Finally, the peak current ratio was calculated to evaluate the recognition efficiency.

Results and Discussion

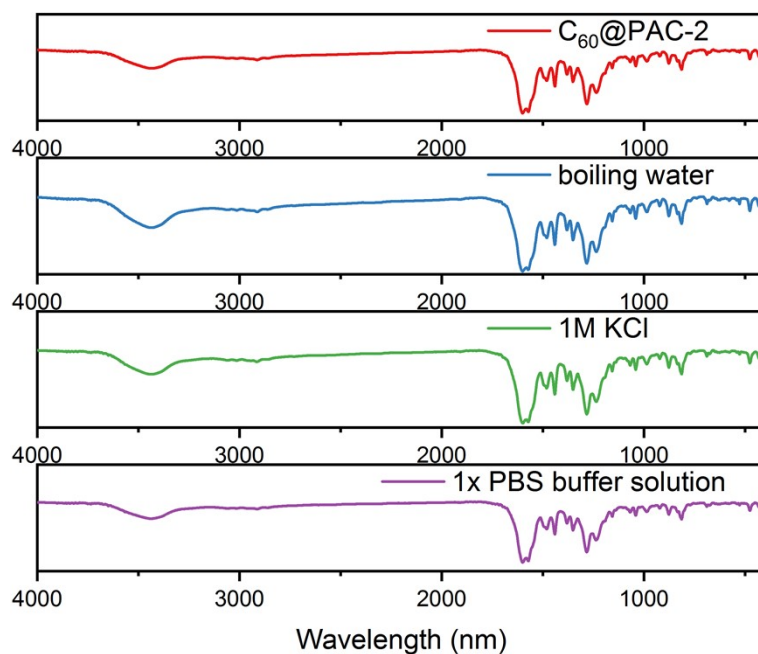


Fig. S1. FTIR spectrum (KBr pellets) of $C_{60}@R-PAC-2$ after soaking under different conditions. FTIR spectrum of the pristine $C_{60}@R-PAC-2$ (Red), under boiling water (blue), 1M KCl (green) and 1 X PBS buffer solution (purple).

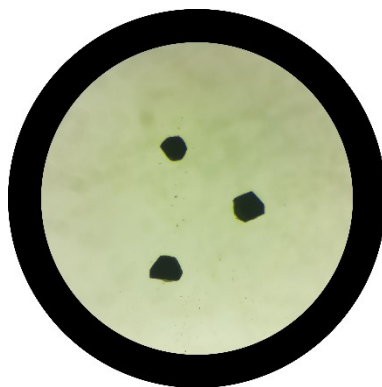


Fig. S2. Photograph of the prepared crystals of $C_{60}@R-PAC-2$.

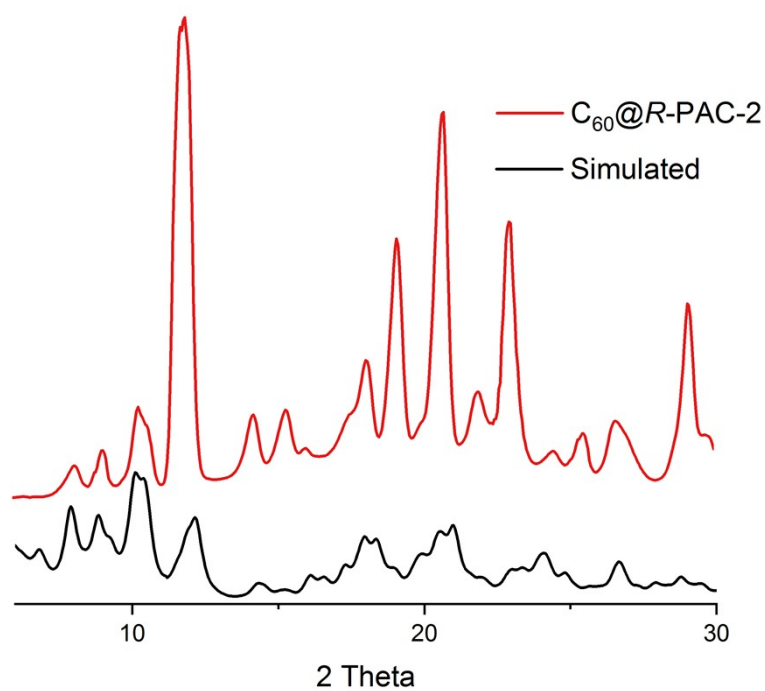


Fig. S3. PXRD patterns of cages. The synthesized (red line) and simulated one of $C_{60}@R-PAC-2$ (black line).

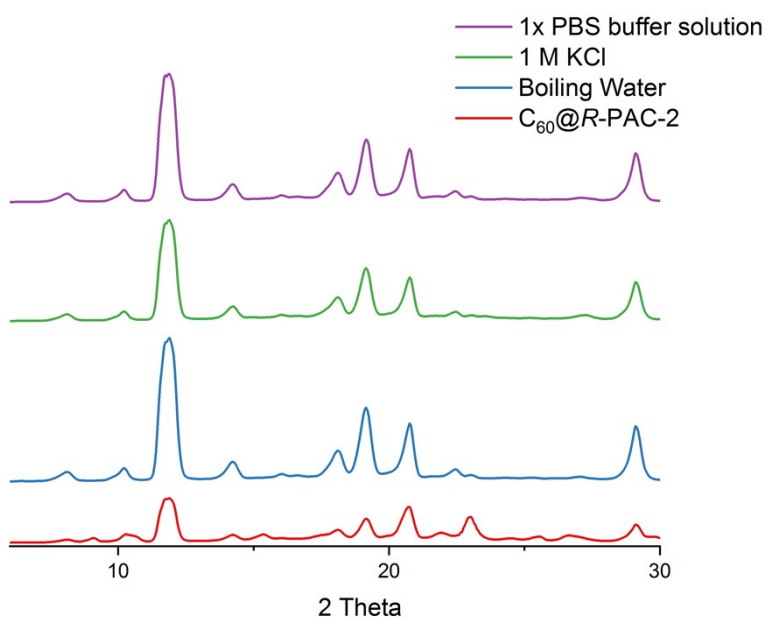


Fig. S4. PXRD patterns of $C_{60}@R-PAC-2$ under different harsh conditions. The the $C_{60}@R-PAC-2$ (red), $C_{60}@R-PAC-2$ under boiling water (blue), 1M KCl (green) and 1 X PBS buffer solution (purple).

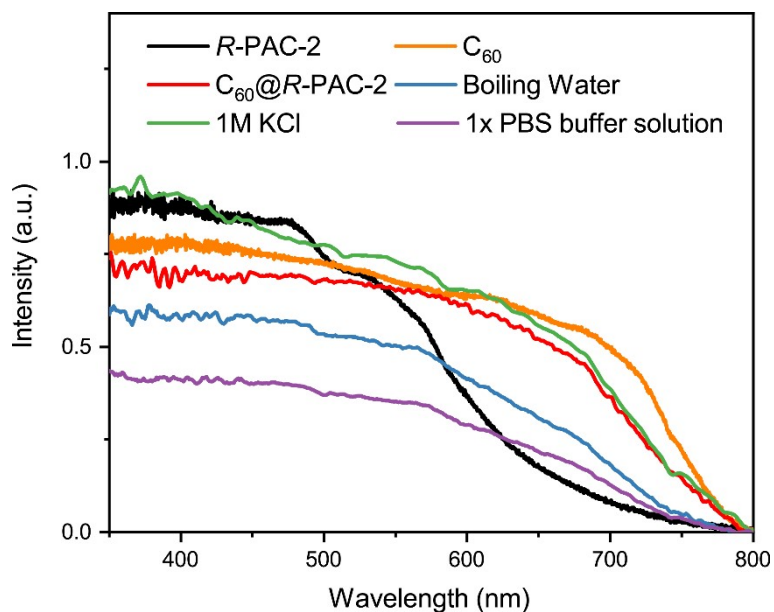


Fig. S5. UV-vis diffuse reflectance spectra of *R*-PAC-2 (black) and C₆₀@*R*-PAC-2 (red). UV-vis diffuse reflectance spectra of the pristine C₆₀@*R*-PAC-2 under boiling water (blue), 1M KCl (green) and 1 X PBS buffer solution (purple).

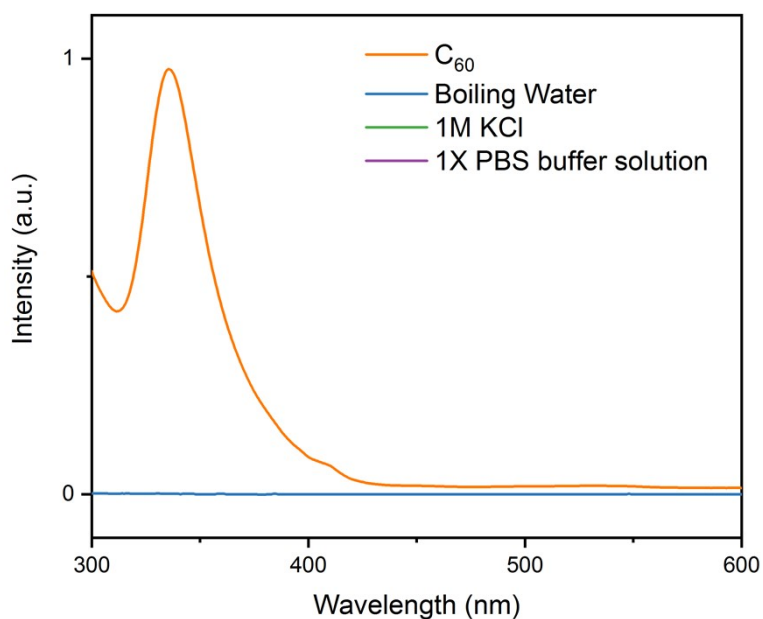


Fig. S6. UV absorption spectra of C₆₀ in toluene (orange). UV absorption spectra of different solution after immersing C₆₀@*R*-PAC-2.

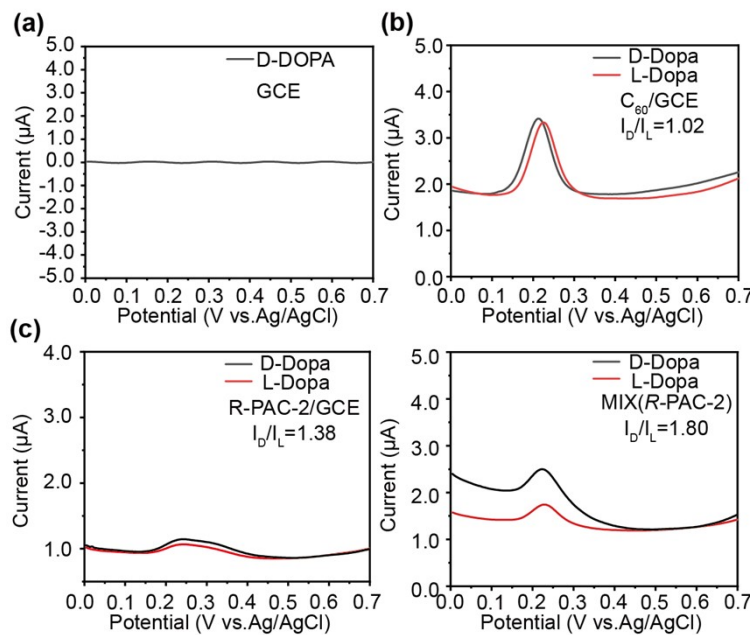


Fig. S7. DPV of (a) GCE, (b) C_{60}/GCE , (c) PAC-2/GCE and (d) MIX in 0.01 M PBS solution containing 0.1 mM D-Dopa or L-Dopa.

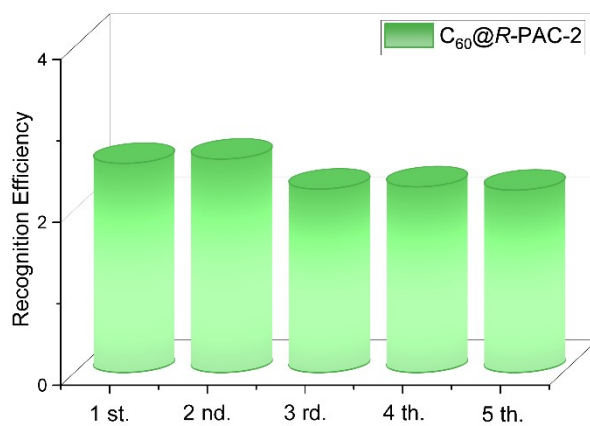


Fig. S8. Repeated electrochemical recognition of DOPA enantiomers by using $\text{C}_{60}@R\text{-PAC-2}/\text{GCE}$ electrode.

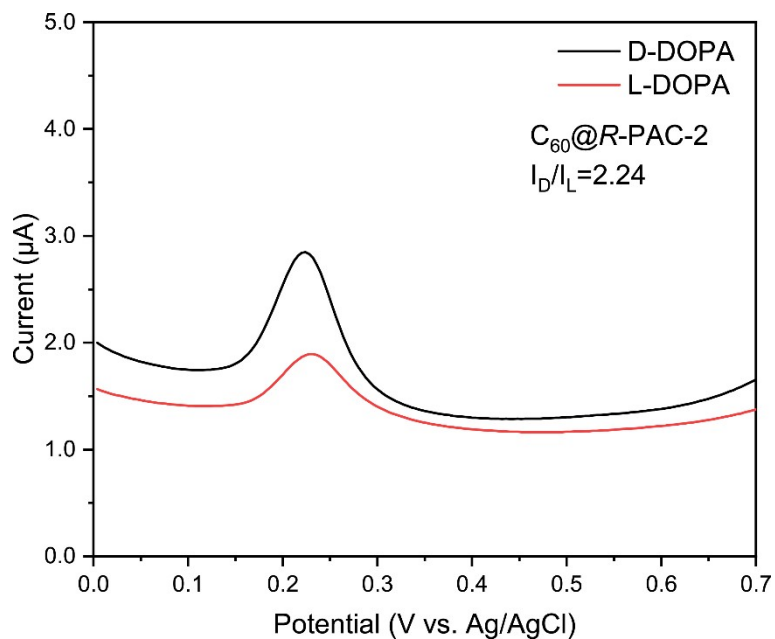


Fig. S9. The stability of the $C_{60}@R-PAC-2/GCE$ sensor was studied after storing for 1 week.

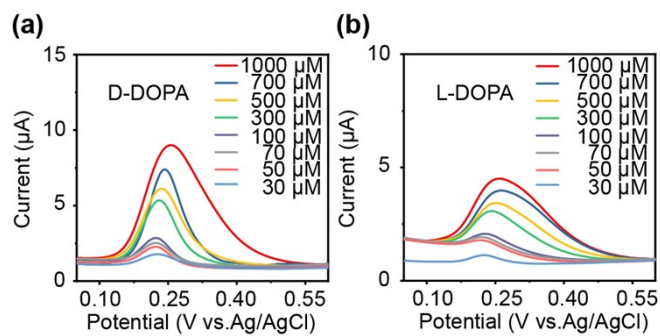


Fig. S10. DPV curves of increased concentrations (30 - 1000 μM) of enantiomers D-DOPA(a) and L-DOPA(b) at the $C_{60}@R-PAC-2/GCE$ electrode.

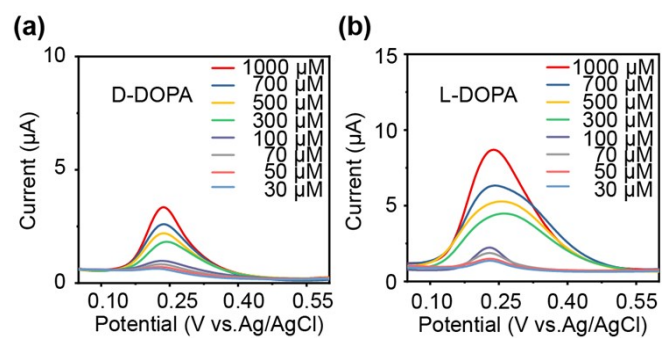


Fig. S11. DPV curves of increased concentrations (30 - 1000 μM) of enantiomers D-DOPA(a) and L-DOPA(b) at the $\text{C}_{60}@S\text{-PAC-2}/\text{GCE}$ electrode.

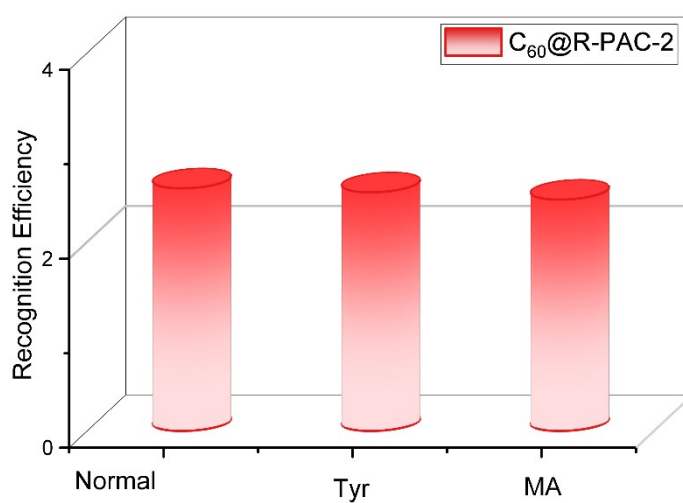


Fig. S12. The detection performance of chiral sensor $\text{C}_{60}@R\text{-PAC-2}$ for interfering organic molecules.

Supplementary Table 1. Summary of DOPA Chiral Sensors

Modifier	Method	Recognition difference	LOD	Ref.
AuND/GCE	DPV	2.33	2.5 μ M	1
SWCNTs-EDA	CV	2.55	-	2
M-(6,5)-SWCNT	DPV	2.05	-	3
P-(6,5)-SWCNT	DPV	1.90	-	3
β -CD/MWCNTs-IL	DPV	1.51	1.2 nM	4
Poly-lysine	CV/DPV	1.56	0.17 μ M	5
L-tryptophan / Graphene / Pt NPs	DPV	1.60	1.7 10^{-8} M	6
cSWCNTs	SWV	1.4	-	7
GNPs/cSWCNTs	SWV	2.1	-	8
PLL/GCE	DPV	1.60	0.33 μ M	5
P-SWCNTs/CFE	DPV	1.4	-	9
CdSe/ZnS QDs-PADP	Fluorescence	2.49	-	10
C ₆₀ @R-PAC-2	DPV	2.6	0.2 μ M	This work

Supplementary References

1. H. Lian, S. Huang, X. Wei, J. Guo, X. Sun and B. Liu, *Talanta*, 2020, **210**, 120654.
2. H. Zhu, F. Chang and Z. Zhu, *Talanta*, 2017, **166**, 70-74.
3. C. Pu, Y. Xu, Q. Liu, A. Zhu and G. Shi, *Anal. Chem.*, 2019, **91**, 3015-3020.
4. Y. Chen, Y. Huang, D. Guo, C. Chen, Q. Wang and Y. Fu, *J. Solid State Electrochem.*, 2014, **18**, 3463-3469.
5. Y. Huang, Q. Han, Q. Zhang, L. Guo, D. Guo and Y. Fu, *Electrochim. Acta*, 2013, **113**, 564-569.
6. Y. Chen, J. Xu, C. Chen, D. Guo and Y. Fu, *New J. Chem.*, 2015, **39**, 6919-6924.
7. L. Chen, F. Chang, L. Meng, M. Li and Z. Zhu, *Analyst*, 2014, **139**, 2243-2248.
8. L. Chen, S. Liu, F. Chang, X. Xie and Z. Zhu, *Electroanalysis*, 2017, **29**, 955-959.
9. W. Kuang, H. Luo and Z. Zhu, *Electrochim. Acta*, 2024, **487**, 144162.
10. Z. Li and M. Zhu, *Chem. Commun.*, 2020, **56**, 14541-14552.